Talanta 117 (2013) 55–59

Contents lists available at ScienceDirect

Talanta

journal homepage: www.elsevier.com/locate/talanta

Quantitative determination of calcium, magnesium, and zinc in fingernails by laser-induced breakdown spectroscopy

David A. Rusak*, Ann E. Zeleniak, Jillian L. Obuhosky, Scott M. Holdren, Craig A. Noldy

Department of Chemistry, University of Scranton, Scranton, PA 18510, USA

ARTICLE INFO

Article history:
Received 31 May 2013
Received in revised form
7 August 2013
Accepted 14 August 2013
Available online 30 August 2013

Keywords:
Laser-induced breakdown spectroscopy
Fingernails
Calcium
Magnesium
Zinc

ABSTRACT

Quantitative determination of Ca, Mg, and Zn in fingernails was performed with laser-induced breakdown spectroscopy. Two different methods of producing solid standards for calibration were explored – preparation of keratin pellets and deposition of aqueous solutions to filter papers. Measurements of the temperature and electron density of the plasma produced on keratin pellets, filter paper, and nails were performed, and it was determined that the standards prepared on filter paper gave plasma temperatures and electron densities closer to those observed on the nails. The ablation rate of the filter paper was also more similar to that of the nails. Using calibration curves produced using these filter paper standards, Ca, Mg, and Zn were determined in fingernails of 11 subjects. For comparison, the same samples were digested and atomic absorption was used to determine the same three elements. The differences in results are discussed in light of sample homogeneity and instrumental precision; the best agreement was obtained for determination of Zn. The work suggests that the filter paper method of standard preparation may be appropriate for LIBS analysis of other samples that give relatively low temperature, low electron density plasmas (i.e., polymers).

1. Introduction

The determination of elemental biomarkers in human fingernails and toenails has been investigated by authors in a variety of disciplines using a number of different analytical techniques [1–12]. Most often these experiments have been undertaken in an attempt to correlate concentrations of specific elements with a medical condition [3,5,7–12], or in the interest of assessing environmental exposure to toxic metals [4,6]. Nails are an attractive sample for determination of elemental biomarkers because concentrations of elements excreted in the nail reflect an average over a much larger time scale than those of elements found in urine or blood; once in the nail, these elements are isolated from metabolic processes. Elements that are most commonly determined in nails include Na, K, Ca, Mg, Zn, Ti, Fe, Cu, Pb, Cd, As, Ni, Hg, Al, and Si. For elements present in nails at ppb levels such as Pb, Hg, As, and Cd, digestion of the nails in acid followed by analysis with ICP-MS has been the technique of choice. For elements present at concentrations of ppm, various techniques, including laser-induced breakdown spectroscopy (LIBS) have been employed [2,7–10].

Hosseinimakarem et al. [2] acquired LIBS spectra of human fingernails in the spectral region of 200–800 nm and assigned the observed emission lines. Using discriminant function analysis, they showed correlations between element concentrations and age and gender. Shadman et al. [7] measured emission lines from 13 elements to distinguish fingernails of opium-addicted subjects from healthy subjects. Hamzaoui et al. [10] measured the relative concentrations of Ca, Na, and K in nails in an attempt to use LIBS as a tool for diagnosis of onychomycosis, a fungal infection of the nail bed. Bahreini et al. [8] determined relative concentrations of Na, K, Ca, Fe, Mg, and Si in fingernails of subjects with osteoporosis. The same authors also investigated the possibility of using LIBS of fingernails to diagnose hyper- and hypothyroidism [9].

All of these studies were either qualitative or semi-quantitative; they determined only relative concentrations of the elements investigated. LIBS is well-suited to these types of studies because they can rely on intensity ratios which can be measured with greater precision than absolute intensities. Historically, it has been proven difficult to create matrix-matched, homogeneous, solid standards to be used to generate LIBS calibration curves based on absolute line intensities [13]. Moreover, the method of standard addition, commonly used to overcome the matrix matching problem, is far more difficult to implement with solid samples than with solutions.

In this work, quantitative determination of Ca, Mg, and Zn in nails by LIBS was investigated. These elements were chosen

* Corresponding author. Tel.: +1 570 941 6338; fax: +1 570 941 7510.
E-mail address: david.rusak@scranton.edu (D.A. Rusak).

0039-9140/$ - see front matter © 2013 Elsevier B.V. All rights reserved.
http://dx.doi.org/10.1016/j.talanta.2013.08.022

because of their relevance to osteoporosis – it is believed that Zn and Mg inhibit calcification and bone growth and aid in the disease progression [3,7,8] - and because of the their prominence in the literature. Karita et al., for example, have determined concentrations of these elements in nails using acid digestion and atomic absorption (AA) and reported concentration ranges of approximately 50–250 ppm for Mg and Zn and 80–1650 ppm for Ca [3].

2. Materials and methods

2.1. Equipment

We used a Q-switched Nd:YAG laser (Ultra CFR, Big Laser Inc., Bozeman, MT) operating at 1064 nm with a pulse width of 7 ns. The 5 mm diameter beam was focused with a 100 mm focal length lens onto the surface of the sample. The pulse energy was 20 mJ and the energy density at the sample surface was 10^{10} W cm^{-2}. The emission from the laser-induced plasma was focused by a 50 mm diameter f/2 lens into a 0.30 m spectrometer (Spectra Pro 2300i, Princeton Instruments/Acton Research, Acton, MA) and dispersed with either a 2400 line/mm holographic grating optimized for UV or a 1800 line/mm grating blazed at 500 nm. The spectra were acquired with an intensified charge-coupled device (ICCD) camera (PI-Max, Princeton Instruments Inc., Trenton, NJ). The delay between firing of the laser and the image acquisition was 1.0 μs and the gate width was 10 μs.

2.2. Emission lines

A survey of the LIBS spectra between 200 and 800 nm was taken on a fingernail sample. Using the NIST atomic lines database, emission lines from nine different elements – Na, K, Mg, Ca, Zn, Ti, Al, Si, and H were identified. The line assignments were confirmed by acquiring LIBS spectra of salts or pure metals of these elements (except H). Next, strong emission lines of Ca, Mg, and Zn that were free from interferences and therefore appeared to be good candidates for quantification were identified. Finally, a series of Ti lines that appeared in a single spectral window (~30 nm) and arose from different upper energy levels were identified as good candidates for measurement of plasma temperature. A summary of emission lines chosen for this work and their relevant spectroscopic parameters appears in Table 1.

2.3. Standards

Two different methods of producing standards for calibration were explored. In the first method, solid standards were prepared by mixing keratin with aqueous solutions containing different concentrations of the elements of interest and drying the samples in a mold to produce a light brown pellet with a glass-like appearance. In the second method, solid standards were made using filter paper as a matrix by depositing aqueous solutions containing different concentrations of the elements of interest to filter papers and drying them in an oven. This technique of using filter paper as a substrate for analysis of liquids by LIBS has been investigated recently by Lee et al. [14]. In our work, the technique was employed to produce the Ca, Mg, and Zn standards for calibration in the interest of analyzing the nails. Measurements of the temperature and electron density of the plasma produced on keratin pellets, filter paper, and nails were made using Boltzmann plots and H_α line widths respectively.

Keratin standards containing Ca at concentrations of 100, 500, 1000, and 5000 ppm, Mg at concentrations of 50, 100, 500, and 1000 ppm, and Zn at concentrations of 50, 100, 500, and 1000 ppm were prepared by combining 2.0 g of keratin powder (Spectrum, New Brunswick, NJ) with 2.0 ml of a solution containing the targeted element at the desired concentration. The mixture was homogenized using a mortar and a pestle and a portion of the mixture was pressed into a small vial cap which served as a cylindrical mold. The surface of the deposited mixture was leveled using a glass rod, and the mixture was allowed to dry in the mold for 48 h to produce the standard. For use in the temperature measurement, another standard containing Ti was prepared by combining 2.0 g of keratin, 2.0 ml of nanopure water, and 10 mg of TiO_2. This mixture was homogenized and dried into a pellet by the same method as others. Although it would have been possible to measure plasma temperature using relative intensities of Ca or Mg lines, Ti provided seven observable emission lines within a single spectral window which led to increased precision in determining the slope of the Boltzmann plot.

In order to create standards using filter paper, the mass of aqueous solution required to wet the paper was determined. Surprisingly, it was found that the filter paper (VWR Grade 413, West Chester, PA) absorbed almost exactly an equal mass of aqueous solution. For example, 10.0 μL of solution wet an area of the filter paper with a diameter of approximately 10 mm. The mass of a 10 mm diameter portion of dry filter paper had a mass of 10.7 mg. Therefore, filter paper standards could be produced by adding 10 μL of aqueous solution containing the target element at the desired concentration to the center of filter papers, marking the boundary of the spot produced on the paper, and allowing the filter papers to air dry. This technique produced a solid standard with approximately the same concentration as that of the aqueous solution. One filter paper was prepared for each element at each concentration. An additional filter paper on which we could observe Ti lines for temperature measurement was prepared by wetting the filter paper with a solution of colloidal TiO_2.

Table 1
A summary of emission lines used in this work with relevant spectroscopic parameters.

Line	Wavelength (nm)	Upper energy level (cm^{-1})	gA (s^{-1})
Ca II	396.8	25,191	
Mg I	285.2	35,051	
Zn I	481.0	53,672	
Ti I	498.2	26,910	8.6×10^8
Ti I	499.1	26,772	6.4×10^8
Ti I	500.0	26,657	4.7×10^8
Ti I	500.7	26,564	3.4×10^8
Ti I	517.4	19,322	2.1×10^7
Ti I	519.3	19,421	2.7×10^7
Ti I	521.0	19,573	3.5×10^7
Hα	656.2	97,492	

2.4. Samples and data acquisition

The samples were fingernail clippings taken from all 10 fingers of 11 different subjects. The samples were referred to by the age and gender of the subject from whom they were taken (i.e., clippings from a 9 year old male were referred to collectively as sample “9M”). In preliminary experiments it has been observed that preparation of the samples by sonication in non-ionic surfactant led to significantly reduced LIBS signals. Therefore, these samples were prepared by simply rinsing with nanopure water. For analysis by LIBS, five laser pulses were used to remove any possible contamination on the surface of the nail, and then five pulses in the same location were accumulated as a single spectrum. This procedure was repeated at five different locations on each nail clipping. The measured intensities used for quantitative

analysis were the average of the background subtracted height of the peak of interest for all of the spectra acquired on nails from a single subject. The standard deviations of the five shot averages were calculated as a means of assessing the combined effects of technique precision and site-to-site variation.

For analysis by atomic absorption (AA), a 70–100 mg sample was digested in 1.0 mL of a 5:1 ratio of 68% HNO_3:70% $HClO_4$ (Fisher, Pittsburgh, PA) over a period of 72 h. After digestion, the samples were diluted to 10.0 mL total volume with nanopure water. These 10.0 mL solutions were analyzed in a Perkin-Elmer AA 300. The blank consisted of 1.0 mL of the 5:1 acid mixture diluted to 10.0 mL total. For Ca, the standard addition technique was employed. A 2.0 mL portion of each initial sample digestion was combined with either 2.0 mL nanopure water, 2.0 mL 50 ppm Ca standard solution, or 2.0 mL 100 ppm Ca standard solution, producing three 4.0 mL samples. These samples were then further diluted by a factor of 2 to allow measurement within the linear dynamic range of the AA. The reported values are the average of three measurements made on each sample and the associated standard deviation.

3. Results and discussion

3.1. Spectra

The LIBS spectra of fingernails in the spectral regions of interest are shown in Fig. 1. Spectrum "a" shows the Ti lines used for temperature calculation, spectrum "b" shows the H_α line used to calculate electron number density, spectrum "c" shows Ca ion lines at 393.4 and 396.8 nm, spectrum "d" shows Mg atom (285.2 nm) and ion (279.6 and 280.3 nm) lines as well as a neighboring Si line, and spectrum "e" shows the Zn atom lines at 472.2 and 481.0 nm. The lines used for calibration are the ones that appear in Table 1.

3.2. Temperature and electron density

A Boltzmann plot for the Ti lines observed on nails is shown in Fig. 2. The corresponding plasma temperature is 4830 ($\pm$ 210) K. Similar plots for the filter paper and the keratin pellet gave temperatures of 4710 ($\pm$ 190) K and 4500 ($\pm$ 200) K respectively. While the accuracy of these absolute temperatures is most likely limited by the accuracy of the transition probabilities, the relative standard deviation is about 5%. A two-tailed t test gives $p=0.48$ for comparison of nails to filter paper, and $p=0.05$ for comparison of nails to keratin pellet. We can conclude that the filter paper gives temperatures that are more similar to those of the nails than the keratin pellet.

Electron number density (n_e) calculated from the width of the H_α lines was also used to assess validity of the standard matrices for analysis of nails. The spectra used for the calculation were acquired in the spectral window shown in Fig. 1. The full width of the line at 656.2 nm was measured and an iterative calculation was performed using the equation $\Delta\lambda_{1/2}=2.50\times10^{-9}\alpha_{1/2}n_e^{2/3}$ with $\alpha_{1/2}$ interpolated from tables by Griem [15]. The resulting electron number densities for plasmas formed on the nails, filter paper, and keratin pellet were 1.0×10^{16}, 8.6×10^{15}, and 7.7×10^{15} respectively. Because the width of the Zn line at 481.0 was also greater than the spectrometer limited line width, this line could also be used to estimate electron number density using $\Delta\lambda_{1/2}=2\omega n_e/10^{16}$ according to Gojani [16]. In this case, using $\omega=0.1$ gives electron densities of 1.2×10^{16}, 1.3×10^{16}, and 1.0×10^{16} cm^{-3} for the nails, filter paper, and keratin pellet respectively. In this case, it can only be concluded that the electron density of the plasmas formed on the nails, filter papers, and keratin pellets were all approximately 10^{16}.

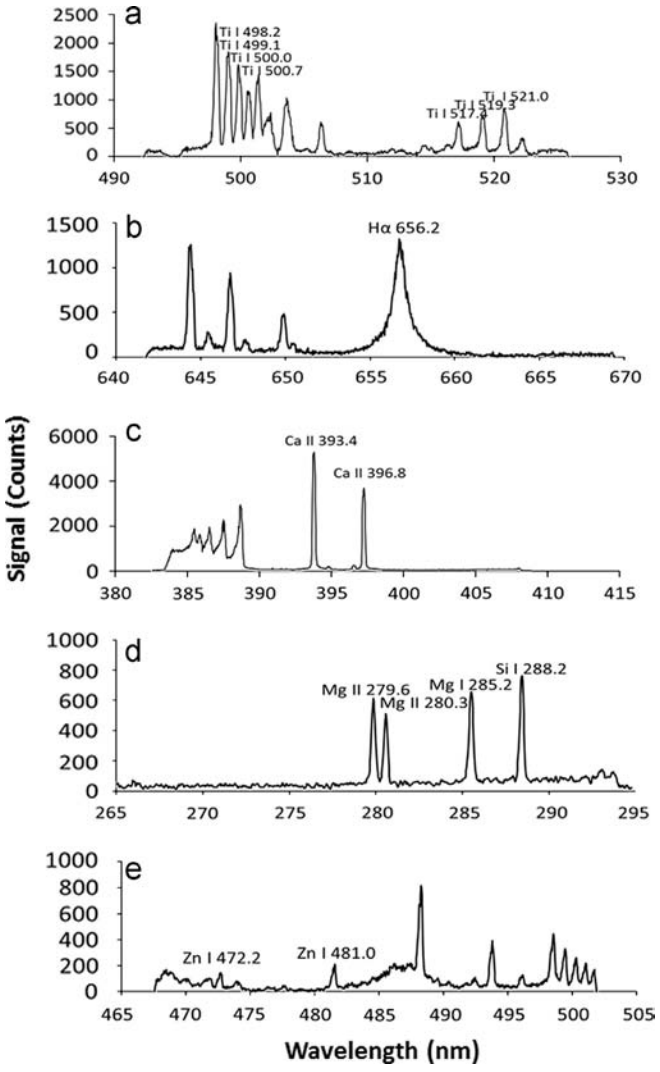

Fig. 1. LIBS spectra of fingernails in the spectral regions of interest.

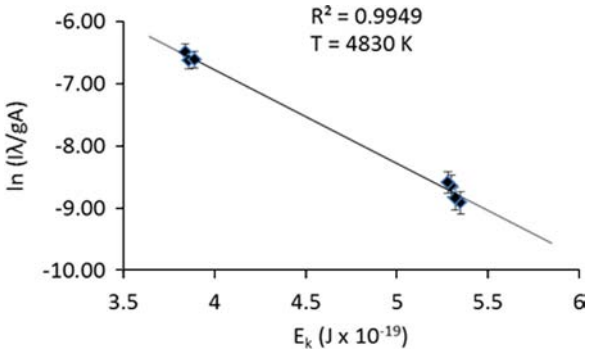

Fig. 2. Boltzmann plot used to determine plasma temperature in plasma formed on a nail.

During these experiments, it was noted that the ablation produced much more damage to the keratin pellets than to the nails or filter paper. While five laser pulses in a single location on nails or filter paper produced damage that was barely visible to the naked eye, a series of five shots in a single location on the keratin produced a crater that was clearly visible. Additionally, on the keratin, the sound that accompanied the plasma formation and the intensity of the emission signals decreased dramatically over the course of five pulses. Using scanning electron microscopy, the

craters formed on the three matrices by five laser pulses in a single location were compared. The results are shown in Fig. 3.

The crater in the keratin pellet (c) is much more pronounced than the crater in the nail (a), which reveals the layered structure of the nail plate, or the filter paper (b), which shows only a few broken fibers. It may also explain the rapid decrease in emission intensity; as the plasma forms in a deeper crater, a significant portion of the emission is unable to be collected. This in turn may be responsible for the decrease in plasma temperature observed. It is interesting to note that although the chemical composition of the nails is almost entirely keratin, the behavior of nails with respect to laser ablation is very different from that of pressed keratin pellets. Differences in supramolecular structure are certainly one possible explanation.

Ultimately, filter paper, keratin pellets and fingernails were similar with respect to electron number densities of the plasma, but filter paper behaved more like nails with respect to plasma temperature and ablation than did keratin pellets. For this reason, the filter paper standard technique was used to generate all the calibration curves used for quantitative analysis of the nails.

3.3. Calibration

Fig. 4 shows the calibration curves produced by LIBS on the filter paper standards for Ca (a), Mg (b), and Zn (c). The error bars correspond to the standard deviations of the signal acquired as five pulse averages in five different locations on the paper.

Here we note that although resonance lines of Ca (Ca II 396.8 nm) and Mg (Mg I 285.2 nm) are used for calibration, there is no evidence of self-absorption even at 5000 ppm Ca. The peaks exhibit no "flat-tops" or depressions at their maxima and the calibration curves are described nicely by linear fits – $R^2=0.9987$ for Ca and $R^2=0.9904$ for Mg. In fact, the only calibration data that suggest the possibility of self-absorption is for the Zn calibration curve which appears to decrease in slope as concentration increases. However, the line used for this calibration (Zn I 481.0 nm) is a non-resonant line and the calibration curve extends only to 1000 ppm. Under these conditions, self-absorption is not likely to be an issue [17].

3.4. Determination of Ca, Mg, and Zn

Table 2 shows the concentration of Ca, Mg, and Zn determined by LIBS using the filter paper calibration technique and determined by acid digestion and analysis by AA. For LIBS, the numbers in parentheses are the standard deviation of the concentration determined from the average of five pulses at five different locations on all 10 nails. For AA, the numbers in parentheses are the standard deviation of three different determinations using nail clippings taken from the same subject. The sample identifiers refer to age and gender. Samples "49F 1" and "49F 2" are taken from two different 49 year old females.

The determined concentrations of Ca, Mg, and Zn fall within the (admittedly large) range found in the literature. Calcium in healthy human nails has been found at concentrations ranging from less than 100 ppm [3] to over 18,000 ppm [18]. Zinc has been

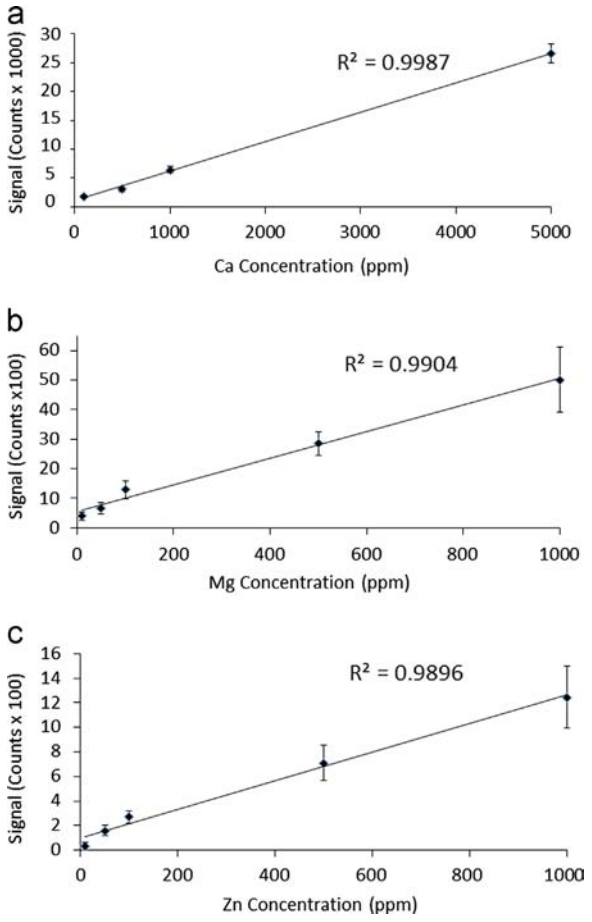

Fig. 4. The calibration curves produced by LIBS on filter paper standards.

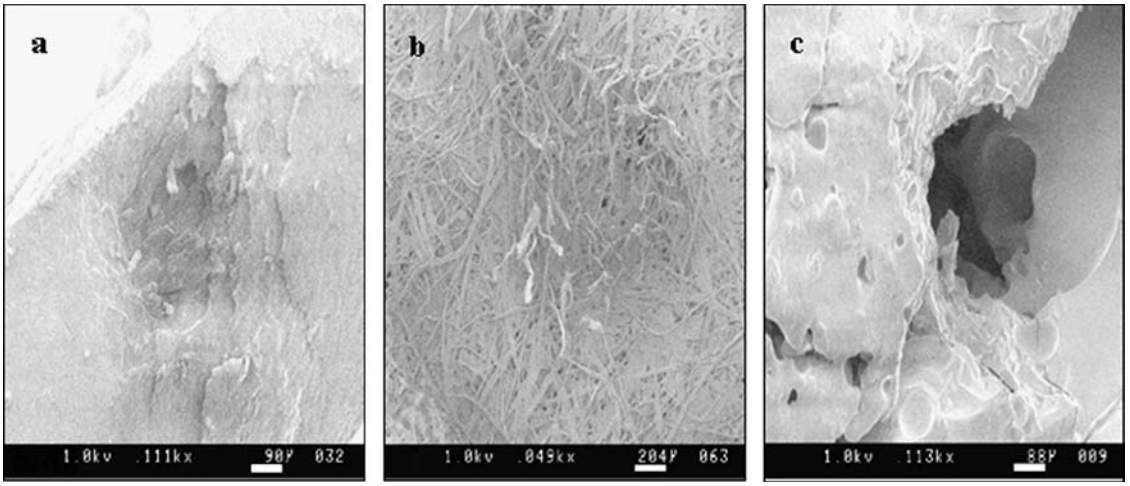

Fig. 3. Scanning electron micrographs of the craters formed by five pulses in a single location on fingernail (a), filter paper (b), and keratin pellet (c).

Table 2
Concentration of Ca, Mg, and Zn determined in nails by LIBS and by AA.

Technique	LIBS/Filter paper (ppm)			AA (ppm)		
Sample/Element	Ca	Mg	Zn	Ca	Mg	Zn
5M	1240 (±144)	141 (±7)	114 (±14)	1840 (±118)	33 (±5)	263 (±16)
10M	1961 (±594)	148 (±5)	106 (±21)	1324 (±89)	47 (±8)	164 (±10)
21M	2564 (±1197)	142 (±4)	116 (±31)	1492 (±97)	100 (±15)	99 (±16)
30F	1322 (±763)	148 (±4)	101 (±20)	671 (±46)	34 (±4)	84 (±15)
33F	1009 (±501)	141 (±8)	88 (±17)	1329 (±80)	59 (±14)	144 (±19)
36M	3043 (±1612)	152 (±8)	106 (±18)	1462 (±82)	53 (±8)	127 (±18)
49F1	1099 (±367)	135 (±4)	113 (±28)	1354 (±80)	61 (±7)	138 (±18)
49F2	1552 (±270)	155 (±6)	95 (±14)	1376 (±88)	74 (±13)	129 (±18)
53M	1240 (±144)	141 (±7)	114 (±14)	1332 (±85)	54 (±11)	111 (±17)
61F	1843 (±828)	143 (±5)	107 (±13)	1339 (±85)	61 (±22)	150 (±19)
67M	1387 (±219)	135 (±3)	119 (±35)	1586 (±99)	64 (±12)	115 (±17)

determined at 40–7000 ppm, the higher values being found in workers at a zinc smelting operation [18], and magnesium has been determined at 50–250 ppm [3]. For our determinations of Ca, the relative standard deviation (RSD) obtained by LIBS was 10–50%. In contrast, the RSD for Ca determined by AA was 5–10%. One explanation for this difference is that the LIBS measurements include contributions from sample inhomogeneity or site-to-site variation in Ca concentration that does not affect the AA experiment. Because AA was used to analyze over 70 mg of nail, this result represents the concentration of the bulk. In comparison, LIBS analyzes only nanograms of sample, and gives a concentration at the surface of the nail in a particular 0.01 mm^2 location. Inhomogeneous Ca distribution in healthy nails has been shown by Shin and Song in their secondary ion mass spectrometry experiment [19].

Concentrations of Mg determined by LIBS had better precision (~5% RSD) and were significantly higher than those determined by AA. Moreover, the concentrations determined by LIBS were found to be almost identical in all the nail samples. This data suggests that Mg concentration is greater at the surface of the nail than in the bulk (possibly because of absorption from the environment). The precision of the LIBS measurement also implies that, at the surface, the distribution is more homogeneous for Mg than for Ca.

The agreement between the LIBS data and the AA data was best for Zn. The RSD for both experiments was 15–20% and the majority of samples yielded concentrations by LIBS that were not statistically different from those obtained by AA at 95% confidence level. In this case, the similar concentrations are a function of the precision of the measurement, the homogeneity of the sample, and the sensitivity of the Zn 481.0 nm line.

4. Conclusions

It has been shown that pellets produced from spiked keratin powder do not make suitable standards for analysis of fingernails by LIBS. We suggest that this is because of the supramolecular structure (fibers, supercoils, etc.) of keratin in fingernails. It has also been shown that standards made by depositing aqueous solutions onto filter paper give plasma temperatures, electron densities, and ablation properties that are similar to those observed on nails. Thus, these filter paper standards are more appropriate for use in calibrating the LIBS experiment for analysis of nails, and it is likely that these standards would work well with other samples that yield relatively low temperature, low electron density plasmas (i.e., polymers). Ca, Mg, and Zn have been determined in fingernails and results have been compared to those obtained by AA. Differences in results may be attributed to sample inhomogeneity (either in the surface dimension or the depth dimension) which affects the LIBS experiment and the AA experiment differently because of the difference in the mass of sample analyzed by each technique. In these experiments, the sample inhomogeneity was inherent to the sample. However, it should be noted that inhomogeneity may also be induced by a robust cleaning procedure which reduces concentrations of metals at the surface of the nail and, as a result, decreases LIBS signals. Simply rinsing the sample and allowing a few laser pulses to "clean" the sample before analysis by LIBS gave better results than did cleaning by sonication in a non-ionic surfactant.

References

[1] B.L. Batista, J.L. Rodrigues, J.A. Nunes, L. Tormen, A.J. Curtius, F. Barbosa Jr., Talanta 76 (2008) 575–579.
[2] Z. Hosseinimakarem, S.H. Tavassoli, J. Biomed. Opt. 16 (5) (2011) 057002–1–057002-8.
[3] K. Karita, T. Takano, S. Nakamura, N. Haga, T. Iwaya, J. Trace Elem. Med. Biol. 15 (2001) 36–39.
[4] A. Sukumar, Rev. Environ. Contam. Toxicol. 185 (2006) 141–177.
[5] Y.R. Tang, S.Q. Zhang, Y. Xiong, Y. Zhao, H. Fu, H.P. Zhang, K.M. Xiong., Biol. Trace Elem. Res. 92 (2003) 97–103.
[6] R. Mehra, M. Juneja, J. Biosci. 30 (2) (2005) 253–257.
[7] S. Shadman, M. Bahreini, S.H. Tavassoli, Appl. Opt. 51 (12) (2012) 2004–2011.
[8] M. Bahreini, Z. Hosseinimakarem, S.H. Tavassoli, J. Appl. Phys. 112 (2012) 1–9.
[9] M. Bahreini, S.H. Tavassoli, Lasers Med. Sci. 3 (3) (2012) 127–131.
[10] S. Hamzaoui, R. Khleifia, N. Jaïdane, Z. Ben Lakhdar, Lasers Med. Sci. 26 (2011) 79–83.
[11] M. Nouri, H. Chalian, A. Bahman, H. Mollahajian, M. Ahmadi-Faghih, H. Fakheri, A. Soroush, Arch. Iran. Med. 11 (4) (2008) 392–396.
[12] K. He, Eur. J. Clin. Invest. 41 (1) (2011) 98–102.
[13] A.K. Pathak, R. Kumar, V.K. Singh, R. Agrawal, S. Rai, A.K. Rai, Appl. Spectrosc. Rev. 47 (2012) 14–40.
[14] Y. Lee, S.W. Oh, S.H. Han, Appl. Spectrosc. 66 (12) (2012) 1385–1396.
[15] H.R. Griem, Spectral Line Broadening by Plasmas, Academic Press, New York/London, 1974.
[16] A.B. Gojani, ISRN Spectrosc. (2012) 1–8.
[17] D. Bulajic, M. Corsi, G. Cristoforetti, S. Legnaioli, V. Palleschi, A. Salvetti, E. Tognoni, Spectrochim. Acta B 57 (2002) 339–353.
[18] M. Uo, K. Asakura, E. Watanabe, I. Hayashi, T. Yanagi, H. Shimazu, F. Watari, Nano Biomed. Eng. 2 (2) (2010) 103–106.
[19] J.T. Song, H. Shin, J. Korean Phys. Soc. 57 (5) (2010) 1285–1289.